Industrial Crops & Products 179 (2022) 114655

Contents lists available at ScienceDirect

Industrial Crops & Products

journal homepage: www.elsevier.com/locate/indcrop

Extraction of the wheat straw hemicellulose fraction assisted by commercial endo-xylanases. Role of the accessory enzyme activities

Andrea Rodríguez-Sanz, Clara Fuciños, Ana M. Torrado, María L. Rúa *

Biochemistry Laboratory, CITACA-Agri-Food Research and Transfer Cluster, Campus Auga, University of Vigo, Ourense, Spain

ARTICLE INFO

Keywords:
Lignocellulosic fractionation
Wheat straw
Alkali pre-treatment
Hemicellulose hydrolysis
Enzymatic extraction

ABSTRACT

Wheat straw is a highly promising raw material for bio-refinery strategies. Most of the literature related to lignocellulose fractionation focuses on cellulose purification and hemicellulose solubilization. Pre-treatments for hemicellulose solubilization without the formation of undesired products usually reach low extraction yields, which leaves an important hemicellulose fraction unused. In this work, we propose a mild process for the efficient extraction of the hemicellulose fraction of wheat straw assisted by partial enzymatic hydrolysis with three commercial endo-xylanase cocktails. A first step with alkali at 40 ºC helped to disrupt the lignocellulosic structure and removed 19% of lignin while maintaining most of the hemicellulose in the solid. The enzymatic step enabled reaching extraction yields of 59.8%, 51.9%, and 42.5% with *Ultraflo L*, *Pentopan mono conc,* and *Shearzyme 500L,* respectively. We also discuss the catalytic properties of each endo-xylanase, in particular, their adscription to the GH10 or GH11 glycosyl hydrolase family, and the relevant role of accessory enzymes.

1. Introduction

Over the years, agroindustry residues have received increasing attention as a sustainable source for innovative products with potential applications in food, pharmaceutical, feed formulations, bioenergy, and agricultural purposes. Among the lignocellulosic residues, wheat straw is considered the most promising one for the bio-economy in the European Union due to its composition, highest production volume, and low exploitation (Thorenz et al., 2018).

Lignocellulosic biomass consists of three main components, i.e., cellulose, hemicellulose, and lignin. Hemicelluloses in grasses are composed mainly of xylan, which is a complex heteropolysaccharide consisting of a backbone of β-1,4-linked xylose units with diverse substituents decorations depending on the source (Hernández-Beltrán et al., 2019). Wheat straw xylan can be substituted by side chains of arabinose, uronic acids (glucuronic and galacturonic acid), acetic acid, ferulic acid, and coumaric acid (Ebringerová, 2005; Peng and Wu, 2010) which can cause a steric hindrance for endo-xylanases action in the xylan backbone. In this regard, the relevant effect of accessory enzymes such as β-xylosidase, α-L-arabinofuranosidase, feruloyl esterase, and acetyl esterase plays a key role in arabinoxylan depolymerization. The combined action of these enzymes allows the transformation of xylan into xylose and xylooligosaccharides (XOS) as platforms for the production of bio-based building blocks such as xylitol, furfural and levulinic acid (Choi et al., 2015).

Due to the compacted structure of lignocellulose, pre-treatment steps are necessary for the fractionation and efficient utilization of hemicellulose and cellulose. Previous studies (Pinales-Márquez et al., 2021; Poletto et al., 2020; Robak and Balcerek, 2020) have compiled pre-treatment methods such as hydrothermal pre-treatment, steam explosion, acid pre-treatment, organic solvent pre-treatment, among others. These pre-treatments allow high yields of hemicellulose extraction but they are not exempt of shortcomings. They require harsh temperature conditions and solvent concentration, which result in undesired by-products formation such as acetic acid, furfural, hydroxymethylfurfural (HMF), formic acid, and phenolic compounds. These compounds can further affect the rate of enzymatic hydrolysis or increase final purification costs for using xylose and XOS (Santibáñez

Abbreviations: A, arabinose; ADP, arabinoxylan-derived product; CAE, Cold alkaline extraction; F, furfural; G, glucose; GDP, glucan-derived product; GH, glycoside hydrolase; H, humidity; HMF, hydroxymethylfurfural; pNPA, *p*-nitrophenyl α-L-arabinofuranoside; pNPX, *p*-nitrophenyl β-D-xylopyranoside; M, monomers; MUX, 4-Methylumbelliferyl-β-D-xylopyranoside; SEM, scanning electron microscopy; V, volume; W, weight; WS, wheat straw; WSs_NaOH$_{10}$, residual solid wheat straw after NaOH 10 g/L pre-treatment; WSs_NaOH$_{100}$, residual solid wheat straw after NaOH 100 g/L pre-treatment; X, xylose; XOS, xylooligosaccharides.

* Corresponding author.
E-mail address: mlrua@uvigo.es (M.L. Rúa).

https://doi.org/10.1016/j.indcrop.2022.114655
Received 28 August 2021; Received in revised form 2 February 2022; Accepted 4 February 2022
Available online 18 February 2022

et al., 2021). For instance, by using these types of pre-treatments on wheat straw some studies have been able to solubilize 97.5–97.3% of the hemicellulose but also obtained 4.3–7.4 g/L of furfural and 1.6–4 g/L of acetic acid as residual products (Ilanidis et al., 2021; Tang et al., 2021).

Alternatively, mild alkaline pre-treatments can substitute the above-mentioned harsh pre-treatments. They allow delignification and partial hemicellulose solubilization without the formation of inhibitory compounds (Santibáñez et al., 2021). The type of the basic catalyst, the hydroxyl concentration, and pH influence the pre-treatment performance. Accordingly, treatments are more intense when stronger bases and high concentrations and temperatures are applyed (Pedersen et al., 2010; Svärd et al., 2017). After mild alkaline pre-treatments, the solubilized hemicellulose is usually precipitated with ethanol as a purification step, and then it undergoes enzymatic hydrolysis to produce xylooligosaccharides or xylose. The problem with this technique is that extraction yields are generally lower than those obtained using harsh pre-treatments. They are usually below 50%, irrespective of the NaOH concentration and temperature conditions applied (García et al., 2013; Kontogianni et al., 2019; McIntosh and Vancov, 2011; Ruzene et al., 2008), which then leaves a high hemicellulose content in the residual solid material.

The purpose of this work is to design a process that allows obtaining high hemicellulose extraction yields from wheat straw (WS) by combining a mild alkaline pre-treatment with a further step of enzymatic hydrolysis applied to the pre-treated solid material, rather than the liquid fraction. To achieve this, we performed the following three steps. First, we established the alkali pre-treatment conditions that allowed decreasing the lignin content of the wheat straw with no significant loss on the hemicellulose. Second, we carefully characterized the enzymatic activities on three commercial enzymatic preparations, *Ultraflo L*, *Shearzyme 500 L,* and *Pentopan mono conc,* considering the main endo-xylanase activity, but also the different accessory enzyme activities useful for lignocellulosic material depolymerization. Third, we evaluated the performance of the three endo-xylanase cocktails for the enzymatic extraction of the arabinoxylan from the solid alkaline pre-treated residue.

2. Material and methods

2.1. Materials

Wheat straw biomass was kindly donated by Molifibra Molienda y Granulacion S.L. (Castilla y León, Spain). Enzymes *Ultraflo L*, *Shearzyme 500 L* and *Pentopan mono conc* were kindly provided by Novozymes A/S (Bagsvaerd, Denmark).

Substrates for activity measurement were purchased: arabinoxylan and malt β-glucanase/lichenase assay kit in Megazyme (Wicklow, Ireland) and p-nitrophenyl β-D-xylopyranoside (pNPX), p-nitrophenyl α-L-arabinofuranoside (pNPA) and 4-methylumbelliferyl-β-D-xylopyranoside (MUX) in Sigma (St Louis, MO, USA).

All other chemicals were of the purest grade available.

2.2. Methods

2.2.1. Cold alkaline extraction (CAE) pre-treatment

The particle size of the raw wheat straw was reduced in a M 20 Universal mill (IKA Labortechnik, Germany). We obtained variable sizes less than 3 cm long (Fig. 1 A). Pre-treatment was carried out for 90 min at 40 ºC and 340 rpm in an orbital incubator KS 4000 ic control (IKA Labortechnik, Germany), with a 1:14 wheat straw:liquid ratio (w/v). Two alkali concentrations were evaluated: 10 g/L and 100 g/L NaOH. After pre-treatment, the solid was neutralized with HCl 37% to pH 5.5–7.0 and washed extensively with distilled water until conductivity < 25 µS/cm. Then, the two pre-treated wheat straw samples were dried in the oven at 70 ºC for characterization and enzymatic hydrolysis. Solid samples resulting from the treatment with 10 g/L and 100 g/L were named WSs_$NaOH_{10}$ and WSs_$NaOH_{100}$, respectively. Liquid fractions resulting from either NaOH treatment were discarded (WSl_$NaOH_{10}$ and WSl_$NaOH_{100}$). Pre-treatment process is summarized in Fig. 1B.

The severity factor (SF) was calculated as follows (Overend and Chornet, 1987) Eq.(1):

$$SF = log\left(t \quad x \quad exp^{\left(\frac{T-100}{14.75}\right)}\right); \tag{1}$$

where t is the incubation time (in min) and T is the temperature (in ºC).

2.2.2. Chemical composition of raw and pre-treated wheat straw

Chemical characterization was done using the NREL standardized method for the determination of structural carbohydrates and lignin in biomass (Sluiter et al., 2012) with some modifications. Briefly, the wheat straw was milled and treated with 72% H_2SO_4 with a 1:10 solid: liquid ratio (w/v) at 30 ºC during 1 h, followed by dilution to 4% H_2SO_4 and second treatment at 121 ºC for 1 h. The sample was filtered through a glass filter funnel and Klason lignin content was quantified gravimetrically. The liquid hydrolysate was filtered by 0.22 µm and analyzed by HPLC using an Agilent 1200 HPLC system (Agilent Technologies, Waldbronn, Germany) equipped with a Transgenomic ICSep ION-300 column (300 ×7.8 mm) (Chromtech, San Jose, CA, USA) with 8.5 mM H_2SO_4 as mobile phase at a flow rate of 0.4 mL/min and temperature 65 ºC. Glucose, xylose, arabinose, acetic acid, galacturonic acid, and glucuronic acid were analyzed with a refractive index detector while furfural (Fur) and hydroxymethylfurfural (HMF) were detected by UV at 250 nm, all of them in the same run. The different compounds were identified and quantified using standard curves, from 5–100 µg/mL. Cellulose and hemicellulose contents of the lignocellulosic substrate were calculated following equations 2 and 3, respectively:

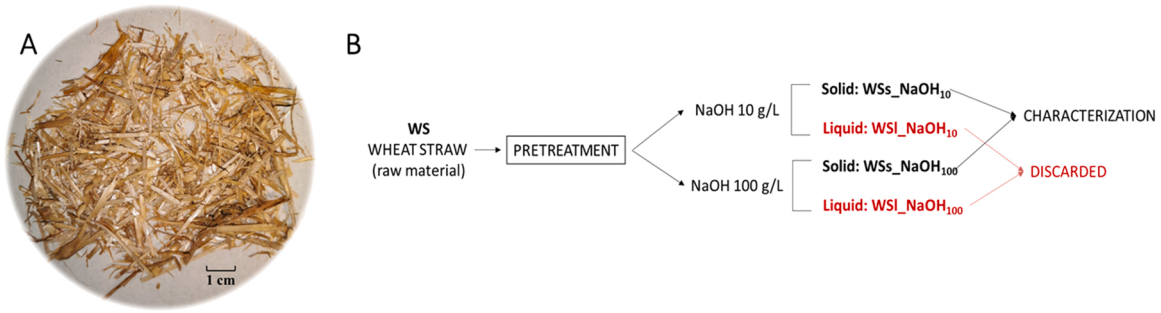

Fig. 1. (A) Chopped raw wheat straw (WS); (B) Flowchart of the pre-treatment protocol at 40 ºC for 90 min using two NaOH concentrations. After NaOH pre-treatment, two fractions were obtained: a solid fraction (WSs) and a liquid fraction (WSl). For further experiments, fraction WSs was used. WSl fraction was discarded.

$$\% \text{ Cellulose} = 100 \times \left(\frac{\frac{([G]+([HMF]\times 1.43)\times V}{1000}}{W \times \frac{100-H}{100}} \right) \times 0.95 \quad (2)$$

$$\% \text{ Hemicellulose} = 100 \times \left(\frac{\frac{([X]+[A]+([F]\times 1.56))\times V}{1000}}{W \times \frac{100-H}{100}} \right) \times 0.94 \quad (3)$$

[G], *[X]*, and *[A]* are the concentration of glucose, xylose, and arabinose (in g/L) quantified by HPLC after the acid treatment. *[HMF]* and *[F]* are the concentrations of hydroxymethylfurfural and furfural (expressed in g/L) considered as the glucose and xylose degradation produced by the treatment applied during the characterization. Thus, correction factors were used to transform HMF to glucose (1.43) and furfural to xylose (1.56). *W* refers to wheat straw weight (expressed in g), *V* refers to the reaction volume (expressed in mL) and *H* refers to the water content (expressed in % of wet weight). 0.95 and 0.94 are correction factors for the water release in the glycosidic bond formation.

For the determination of esterified ferulic and coumaric acids, an alkaline treatment with 0.5 M NaOH (1:30 solid:liquid ratio (w/v)) at 50 ºC for 4 h was performed. Then, the mixture was acidified to pH 5 with 1 M HCl and was centrifuged for 10 min at 16,000g. The supernatant was recovered and diluted 1:1 with MeOH, centrifuged for 5 min, and filtered. The filtrate was analyzed by HPLC using Luna C18 column (150 ×4.6 mm) (Phenomenex, Alcobendas, Spain) following the method described by Saulnier et al. (1999). Standard curves from 12.5–500 μg/mL were used for ferulic and coumaric identification and quantification.

2.2.3. Protein determination

Protein concentrations were measured by Pierce BCA Protein Assay Kit (Pierce, Rockford, IL) with bovine serum albumin (BSA) as the standard.

2.2.4. Enzyme activity assays

Enzyme activity for all tested enzymes was determined in 50 mM citrate-phosphate buffer (pH 5.0) at 40 °C.

Endo-xylanase activity was determined by 3,5-dinitrosalicylic acid (DNS) assay (Bailey et al., 1992) with some changes. Briefly, 180 μL of 1% arabinoxylan were incubated with 20 μL of the diluted enzyme for 20 min. Then 300 μL of DNS were added to stop the reaction. Samples were boiled for 5 min, cooled down on ice, and measured at 540 nm using a microplate scanning spectrophotometer FLUOstar Omega (BMG Labtech, Offenburg, Germany). A xylose standard curve was built from 0–0.5 g/L for xylose quantification. Substrate and diluted enzyme were replaced by 180 μL of xylose solution and 20 μL water, respectively. One unit of endo-xylanase activity was defined as the amount of enzyme that produced 1 μmol of xylose per minute.

β-xylosidase and arabinofuranosidase activities were quantified by measuring the *p*-nitrophenol (pNP) released from *p*-nitrophenyl β-D-xylopyranoside (pNPX) and *p*-nitrophenyl α-L-arabinofuranoside (pNPA) respectively. The reaction mixture containing 100 μL of 25 mM pNPX or pNPA, 800 μL of citrate-phosphate buffer, and 100 μL of the diluted enzyme was incubated for 20 min. The reaction was stopped by immersing the samples on ice and adding 250 μL of 1 M sodium carbonate. Absorbance was determined at 400 nm in a microplate scanning spectrophotometer FLUOstar Omega (BMG Labtech, Offenburg, Germany). A *p*-nitrophenol standard curve from 0–50 μM was used for pNP quantification. The standard mixture contained 100 μL of each pNP solution, 800 μL buffer, 100 μL water, and 250 μL 1 M sodium carbonate. One unit of β-xylosidase and arabinofuranosidase activity was defined as the amount of enzyme that produced 1 μmol of pNP per minute.

β-glucanase/lichenase activity was measured applying the Malt β-glucanase/lichenase assay procedure (MBG4 Method, Megazyme, Wicklow, Ireland), following the protocol supplied by the manufacturer, and using the buffer and temperature conditions mentioned above.

Cellulase activity was measured using the NREL standardized filter paper assay (Adney and Baker, 2008) at the temperature and pH conditions previously defined. Briefly, 50 mg of filter paper strip was placed in 1 mL citrate-phosphate buffer and were incubated with 0,5 mL of the diluted enzyme for 60 min. Then 3 mL of DNS were added to stop the reaction. Samples were boiled for 5 min, cooled down on ice, and centrifuged at 10.000g for 3 min. The supernatant was diluted 12,5 times and measured at 540 nm using a microplate scanning spectrophotometer FLUOstar Omega (BMG Labtech, Offenburg, Germany). Glucose standard curve was built from 2–6.7 g/L and used for glucose quantification following the method protocol. One unit of cellulase activity was defined, in this case, as the amount of enzyme that produced 1 μmol of glucose per minute.

2.2.5. SDS-PAGE, isoelectric focusing, and zymography

Commercial enzymes were analyzed by SDS-PAGE on 12% polyacrylamide gels using a Mini Gel Tank (Fisher Scientific SL, Madrid, Spain), following the method described by Laemmli (1970). Samples were boiled with loading buffer containing 4% (v/v) SDS and 2% (v/v) 2-mercaptoethanol for 5 min. Gels were stained with Coomassie Brillant blue R-250 for bands visualization following standard procedures. Precision plus protein unstained standards (10–250 kDa) (Biorad, Richmond, CA, USA) were used for molecular mass determination.

Zymogram analyses for endo-xylanase activity determination were done after SDS-PAGE using SE260 Mini Vertical Protein Electrophoresis Unit (Hoefer Inc, Holliston, USA) under refrigeration. For the endo-xylanase activity, we used the procedure described by Cano-Ramírez et al. (2017), with some modifications. Briefly, 10% (v/v) polyacrylamide gels were prepared including 0.5% (w/v) arabinoxylan. Electrophoresis was carried out as usual. Then, enzymes were refolded by washing the gel with 2.5% (v/v) Triton X-100 in 50 mM citrate-phosphate buffer (pH 5.0) for 30 min. Afterward, gels were changed to 50 mM citrate-phosphate buffer (pH 5.0), heated at 40 ºC for 45 min, washed again with 0.1 M Tris-HCl (pH 8) for 10 min, and finally stained with 0.1% (w/v) Congo red. The background was turned blue with 1 N HCl. Enzymatic activity was visualized as clear zones.

Before denaturing electrophoresis, samples were diluted in the usual loading buffer and boiled for 2 min. When native electrophoresis was performed, samples diluted in loading buffer without SDS and 2-mercaptoethanol were incubated for 5 min at 40 ºC. In both cases, 1.5 units of endo-xylanase activity (measured as is described in enzyme activity assay method) were loaded onto the gel.

Isoelectric focusing (IEF) was performed using Novex pH 3–10 IEF Protein gels (Fisher Scientific SL, Madrid, Spain) following the manufacturers' specifications. Samples were diluted in sample buffer (20 mM lysine, 20 mM arginine, and 15% (v/v) glycerol) and loaded onto gels. For protein detection, gels were incubated in 12% (w/v) trichloroacetic acid for 30 min, washed with plenty of water, and stained with Coomassie Blue R-250 for 15 min for bands visualization. Isoelectric point was determined with IEF marker 3–10 (Fisher Scientific SL, Madrid, Spain).

β-xylanase activity on IEF gels was visualized as in Yan et al. (2008). Briefly, after electrophoresis, gels were washed twice with 25% (v/v) 2-propanol for 15 min and four times (8 min each) with 50 mM citrate-phosphate buffer (pH 5.0). Afterward, gels were incubated at 40 ºC for 30 min in a solution of 40 μM 4-methylumbelliferyl-β-D-xylopyranoside (MUX) prepared in the previous buffer. Active bands were visualized under UV light.

2.2.6. Enzymatic hydrolysis

Enzymatic hydrolysis of the solid pre-treated wheat straw was carried out with three enzymatic cocktails (*Ultraflo L*, *Shearzyme 500 L*, and *Pentopan mono conc*) at the same pH and temperature at which the enzymatic activity with the standard substrates was determined (pH 5.0

and 40 ºC). The reaction mixture lies in 42 mL buffer containing 1 g of pre-treated wheat straw (WSs_$NaOH_{10}$) and 200 U of endo-xylanase activity. Before adding the enzyme solution, the straw was sterilized for 1 h at 100 ºC. The enzymatic reaction was carried out in an orbital incubator KS 4000 ic control (IKA Labortechnik, Germany) at 230 rpm for 54 h. Aliquots were taken periodically, incubated 10 min at 100 ºC for enzyme inactivation, centrifuged 5 min at 16,000g, filtered by 0.22 μm and analyzed by Agilent 1200 HPLC system (Agilent Technologies, Waldbronn, Germany) equipped with a Transgenomic ICSep ION-300 column (300 ×7.8 mm) (Chromtech, San Jose, CA, USA) with 8.5 mM H_2SO_4 as mobile phase at a flow rate of 0.4 mL/min and temperature 65 ºC. The compounds were identified and quantified as it was performed in Section 2.2.2 for material characterization. Monomers (M) (glucose, xylose, and arabinose) released by the enzymatic hydrolysis (EH) were directly measured by HPLC. Each monomer was calculated following equation 4. Subsequently, samples were subjected to total hydrolysis treatment with 4% H_2SO_4 at 121 ºC for 1 h. Monomers released by the acid treatment (AT) were measured by HPLC and arabinoxylan-derived (ADP) and glucan-derived products (GDP) were calculated as equations 5 and 6, respectively.

$$mg \Big/ g\ Monomers = \left([M]_{EH}\right) \times \frac{V}{W} \quad (4)$$

$$mg \Big/ g\ ADP = \left([X]_{AT} + [A]_{AT} + \left([F]_{AT} \times 1.56\right)\right) \times \frac{V}{W} \quad (5)$$

$$mg \Big/ g\ GDP = \left([G]_{AT} + \left([HMF]_{AT} \times 1.43\right)\right) \times \frac{V}{W} \quad (6)$$

$[M]_{EH}$ is the concentration of glucose, xylose, or arabinose (in mg/mL) quantified by HPLC at the end of the enzymatic hydrolysis, before acid treatment. $[G]_{AT}$, $[X]_{AT}$, and $[A]_{AT}$ are the concentration of glucose, xylose, and arabinose (in mg/mL) quantified by HPLC after the acid treatment. Monomers released in the enzymatic hydrolysis are considered in ADP and GDP equations. $[HMF]_{AT}$ and $[F]_{AT}$ are the concentrations of hydroxymethylfurfural and furfural (expressed in mg/mL) generated from the glucose and xylose degradation produced by the acid treatment applied for polymer quantification. Thus, correction factors were used to transform HMF to glucose (1.43) and furfural to xylose (1.56). W refers to wheat straw weight (expressed in g) and V refers to the reaction volume (expressed in mL).

2.2.7. Scanning Electron Microscopy (SEM) analysis

The solid straw samples to be analyzed were coated with a conductive layer of gold material using sputter coater K550 (Emitech Ltd., Ashford, Kent, UK) before examination by a scanning electron microscope (FEI Quanta 200, FEI Co., Hillsboro, Oreg., U.S.A.) with back-scattered electrons detector. The SEM was operated at 15 kV and magnification of 200 × (CACTI, University of Vigo, Spain).

3. Results and discussion

3.1. Chemical composition and pre-treatment

Lignocelullosic material is composed mainly by cellulose, hemicellulose, and lignin (Hernández-Beltrán et al., 2019). The relative composition of these three fractions and the chemical composition of hemicellulose and lignin depend on the biomass type, plant variety, cultivation, and physiological state. The composition described for wheat straw was: 32–41% cellulose, 22–28% hemicellulose, and 20–22% lignin (Santibáñez et al., 2021). The chemical composition of the raw wheat straw (WS) used in this study is shown in Table 1. The content in cellulose and hemicellulose was similar to those previously described, i.e., 35.5% and 27.2%, respectively, while the lignin content was slightly higher (25.1%). The hemicellulose of the raw material was composed mainly of xylose, with substitutions of acetic acid (15.2%), arabinose (9.7%), galacturonic acid (<2%), glucuronic acid (<2%), ferulic acid (<1%) and coumaric acid (<1%).

Table 1
Composition of solid wheat straw before and after alkaline pre-treatment at 40 ºC for 90 min, expressed as relative % of dry wheat straw.

Pre-treatment	Composition (%)[a]		
	Cellulose	Hemicellulose[b]	Klason Lignin
WS	35.5 ± 0.1^{A}	25.2 ± 0.1^{A}	25.1 ± 0.4^{A}
WSs_$NaOH_{10}$	40.6 ± 1.6^{B}	26.7 ± 1.1^{A}	20.3 ± 0.4^{B}
WSs_$NaOH_{100}$	57.7 ± 2.9^{C}	16.8 ± 1.0^{B}	16.3 ± 1.3^{C}

^{A,B,C} Different capital letters indicate significant differences ($p \leq 0,05$) between samples in the same column

[a] Composition in dry matter expressed as mean ± standard deviation (n = 3).

[b] Considered as arabinoxylan, quantified as it was mentioned in the material and method section.

For lignocellulose biomass enzymatic fractionation, the disruption of the cross-linked compact matrix is an important step for improving enzyme accessibility. A large number of pre-treatment methods have been previously studied. Particularly, alkali pre-treatment using mild conditions shows high efficiency for grass biomass without undesired by-products production. It works by disrupting the ester bonds cross-linking lignin and xylan through ferulate moieties, and xylan-xylan cross-linking mediated by diferulate moieties. As a result, lignin and hemicellulose are partially solubilized, while the solid pre-treated material increases its relative content in cellulose and hemicellulose regarding the raw material (Hernández-Beltrán et al., 2019). Additionally, a fraction of the solubilized lignin can precipitate on the surface of the solid material during the cooling after the pre-treatment. This depends on the solubility of the product with temperature.

To evaluate the lignin and hemicellulose solubilization in wheat straw we tested two different NaOH concentrations. The pre-treatment was carried out with 10 g/L and 100 g/L sodium hydroxide for 90 min at mild temperature (40 ºC) to reduce energy costs and corrosion. The calculated severity factor (SF=0.2) for the two pre-treatments was much lower than other pre-treatments described for the same material (SF>2.7) at higher temperatures (Eisenhuber et al., 2013). Previous studies have noticed that the more severe pre-treatment conditions, the higher is the material modification. Accordingly, less delignification and hemicellulose depolymerization was expected (Eisenhuber et al., 2013; Ewunie et al., 2021; Pedersen et al., 2010).

Despite it, the lignin content of the wheat straw decreased with the alkali pre-treatment, from 25.1% in WS to 20.3% and 16.3% at the lowest (WSs_$NaOH_{10}$) and highest (WSs_$NaOH_{100}$) NaOH concentration, respectively (Table 1). Cellulose enrichment was produced in the solid with both pre-treatments, increasing from 35.5% to 40.6% and 57.7%, respectively. Regarding hemicellulose, the content in the solid material pre-treated with 100 g/L NaOH decreased only 33.5%. This value was significantly lower than those previously reported with the mildest treatment applied by Eisenhuber et al. (2013) (SF 2.77), where less than 25% of the total hemicellulose remained in the solid treated wheat straw. In the case of the solid WSs_$NaOH_{10}$, no significant changes were observed in the hemicellulose content.

These results show that as well as the severity factor, the NaOH concentration is highly relevant even at mild temperature conditions. In fact, Gao et al. (2021) described an exponential relationship between hemicellulose and lignin removal and NaOH concentration when wheat straw was subjected to mechanical-NaOH pre-treatments at 35 ºC.

As previously mentioned, the main advantage of using alkali pre-treatment under mild conditions is that the production of undesired compounds is prevented. In order to further confirm this, furfural and HMF production were analyzed and, as expected, they were not detected (data not shown).

Phenolic compounds and carboxylic acids in the WS and solid pre-treated materials (WSs_$NaOH_{10}$ and WSs_$NaOH_{100}$) have been also

evaluated as these groups are sensitive to alkaline conditions (Linares-Pasten et al., 2016). That is, previous studies have reported the influence of 5-O-feruloylated and 5-O-p-coumaroylated α-1,3 arabinosyl substitutions in the xylan-lignin interaction, which indicates lignin linkages (Terrett and Dupree, 2019). As shown in Table 2, the content of feruloyl, coumaroyl, and acetyl residues decreased after the alkali pre-treatment. Ferulic acid decreased by 73.3% in WSs_NaOH$_{10}$ and 98.2% in WSs_NaOH$_{100}$. For coumaric acid, although the content was negligibly changed in WSs_NaOH$_{10}$, a major decrease was observed under the hardest NaOH pre-treatment. However, the ANOVA analysis of the data suggests that the difference is not statistically significant.

Regarding acetyl groups, the alkali pre-treatment was effective at eliminating them (Table 2). Thus WSs_NaOH$_{10}$ reduced its acetic acid content by 86.7% concerning the initial composition (from acetic acid/xylose ratio = 0.53 in the WS to 0.06 in WSs_NaOH$_{10}$). For WSs_NaOH$_{100}$ acetic acid ramifications were fully eliminated.

Many pre-treatments have been designed for cellulose enrichment and/or hemicellulose solubilization, and the solubilized fraction has been further used as the substrate for enzymatic hydrolysis. Different alkali pre-treatments conditions at atmospheric pressure have allowed extracting 30.6% (Kontogianni et al., 2019), 33% (McIntosh and Vancov, 2011), and 49.3% (Ruzene et al., 2008) of the hemicellulose from the raw wheat straw material. García et al. (2017) obtained a hemicellulose extraction yield of 20.1% by pre-treating the wheat straw with 100 g/L NaOH at 40ºC for 90 min. Applying the same pre-treatment condition, we have extracted 33.5% of the hemicellulose (Table 1). This higher yield could be the result of differences in the material composition, particle size, or agitation.

The percentage of hemicellulose extracted with any of the tested pre-treatments was noticeably insufficient for an efficient process. One way of increasing the extraction yields would be applying more severe conditions, e.g., higher NaOH concentration and/or high temperature/pressure. However, this option would be less cost-efficient or sustainable. We instead focused on the pre-treated solid residue to be subjected to the enzymatic hydrolysis because the pre-treatment tested in this work decreased its lignin content and weakened the lignin-hemicellulose interactions while kept most of the initial arabynoxylan.

Sample WSs_NaOH$_{10}$ was used in the following steps since the pre-treatment with 10 g/L NaOH decreased by 19% the lignin content and maintained unchanging hemicellulose content. In addition, as this pre-treatment decreased the acetyl ramifications of the raw material by 86.7% (Table 2), our final hemicellulose was classified as arabinoxylan. It was composed by xylose, with ramifications of arabinose (9.9%), acetic acid (3.1%), galacturonic acid (< 2%), glucuronic acid (< 2%), coumaric acid (< 1%) and ferulic acid (< 0.3%).

3.2. Inner structure analysis of raw and pre-treated wheat straw by SEM

To evaluate qualitative modifications produced by the pre-treatments, we assess the changes in the surface morphology of the raw and pre-treated wheat straw by SEM. Fig. 2 shows electron micrographs of untreated (WS (A)) and pre-treated wheat straw (WSs_NaOH$_{10}$ (B) and WSs_NaOH$_{100}$ (C)). Untreated material shows a compact and highly ordered structure while pre-treated solid samples have modifications and disruptions in their structure. Additionally, samples from both treatments show pores, but they tend to be more pronounced in WSs_NaOH$_{100}$.

Spherical-shaped structures, which were clearly observed in the WS (Fig. 2A) have been previously identified as lignin deposits (Kristensen et al., 2008). These structures were smaller and less frequently observed in samples WSs_NaOH$_{10}$ (Fig. 2B) and almost absent in WSs_NaOH$_{100}$ (Fig. 2C). These qualitative analyses gave us a visual indication of lignin removal and material structure disruption triggered by the alkali pre-treatments.

These observations together with the chemical composition changes in WSs_NaOH$_{10}$ described above suggest that enzyme access to the scissile bonds has been significantly improved, and therefore high yields on hemicellulose extraction are expected.

3.3. Enzymatic cocktails characterization

For the complete heteroxylan degradation, different xylanolytic activities are required (Fig. 3). Endo-xylanase (EC 3.2.1.8) activity is the most important for xylan degradation, followed by β-xylosidase (EC 3.2.1.37). Xylanase cleaves the xylan backbone randomly producing short xylooligosaccharides which are hydrolyzed by β-xylosidase to xylose units (Nordberg Karlsson et al., 2018; Rohman et al., 2019).

Substituents in the xylan backbone could produce a steric hindrance to the main-chain cleaving enzyme (Van Dyk and Pletschke, 2012). Following that, and according to our results about the substituents of WSs_NaOH$_{10}$ hemicellulose (analyzed in Section 3.1), activities such as α-L-arabinofuranosidase (EC 3.2.1.55), feruloyl esterase (EC 3.1.1.73), acetyl esterase (EC 3.1.1.72), and β-glucuronidase (EC 3.2.1.139) could improve the xylan hydrolysis into monomeric sugars (Fig. 3).

We used three commercial enzyme preparations (*Ultraflo L*, *Shearzyme 500L*, and *Pentopan mono conc*) that have been previously used for degrading lignocellulosic materials. Table 3 shows basic information for each commercial cocktail, including the main enzyme activities and optimal conditions for activity determination provided by the manufacturers. Table 3 also shows accessory activities that have been identified by several authors in the literature.

According to the manufacturer, the three preparations contain endo-xylanase activity and *Ultraflo L* also contains β-glucanase as main activity. All of them show optimal pHs around neutral or slightly acidic values, and they are active over a broad temperature interval, particularly *Shearzyme 500L*. Apart from that, several papers have reported other activities on these preparations (Table 3). Thus, cellulase, feruloyl esterase, and acetyl esterase are accessory activities for *Ultralfo L* whereas β-glucosidase, amylases, and cellulases have been described for *Shearzyme 500 L*. For *Pentopan mono conc* no other activity apart from endo-xylanase has been reported.

3.3.1. Enzyme activity profile

To evaluate the ability of the selected commercial cocktails to act on a complex matrix, extract and hydrolyze arabinoxylan and release monosaccharides, we measured the activity of the main and accessory enzymes that could be relevant in WSs_NaOH$_{10}$ degradation. To that end, we analyzed the endo-xylanase, β-xylosidase, α-L-

Table 2
Ferulic, coumaric, and acetic acid content of the solid wheat straw before and after alkaline pre-treatments at 40 °C for 90 min, expressed as mg per g of dry wheat straw and as molar ratio to xylose.

Pre-treatment	Composition (mg/g wheat straw)[a]			Molar ratio to xylose		
	Ferulic acid	Coumaric acid	Acetic acid	Ferulic acid	Coumaric acid	Acetic acid
WS	2.81 ± 0.23^{A}	1.92 ± 0.16^{A}	50.12 ± 1.92^{A}	0.01	0.01	0.53
WSs_NaOH$_{10}$	0.75 ± 0.02^{B}	2.01 ± 0.07^{A}	6.59 ± 1.64^{B}	0.00	0.01	0.06
WSs_NaOH$_{100}$	0.05 ± 0.01^{B}	0.39 ± 0.01^{A}	0.00 ± 0.00^{C}	0.00	0.00	0.00

^{A,B,C} Different capital letters indicate significant differences ($p \leq 0,05$) between samples in the same column.
[a] Composition in dry matter expressed as mean ± standard deviation (n = 3)

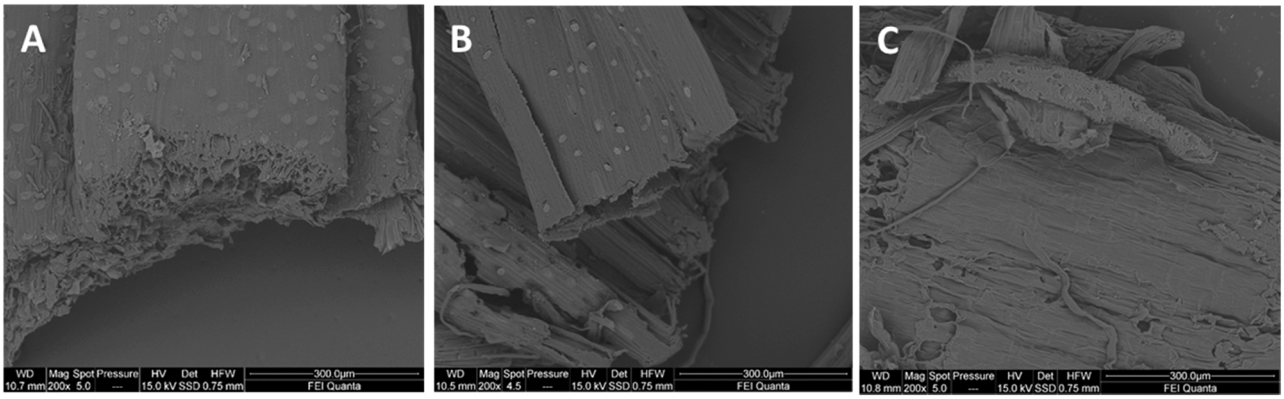

Fig. 2. SEM images of wheat straw before and after alkali pre-treatment. (A) WS; (B) WSs_NaOH$_{10}$; (C) WSs_NaOH$_{100}$. Scale bar of the images is 300 μm. Pre-treatments were performed at 40 ºC for 90 min.

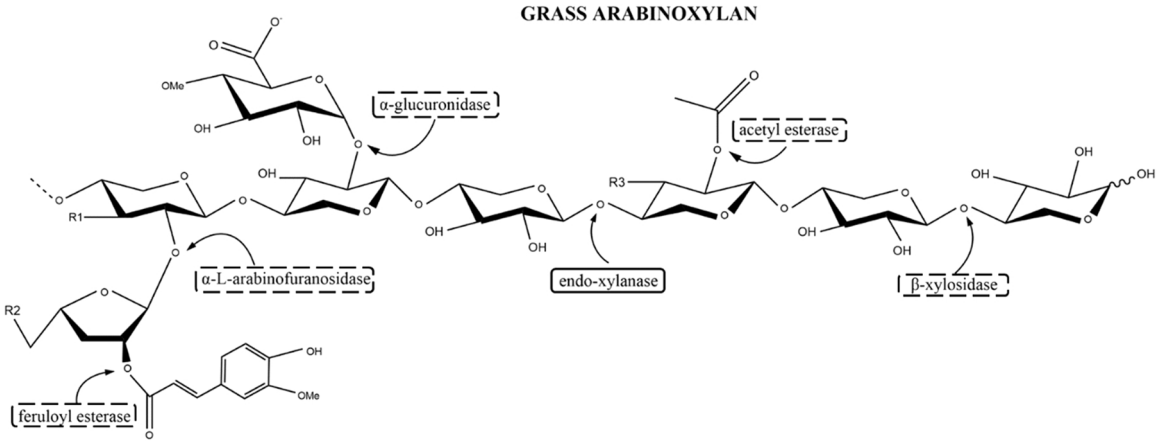

Fig. 3. Hemicellulolytic enzymes and their cleavage sites. The main-chain cleaving enzyme is surrounded by a continuous line and accessory enzymes with a dashed line.
Modified from Shallom and Shoham (2003).

arabinofuranosidase, cellulase, and β-glucanase activities presented in the three commercial enzymes.

Activities were determined as indicated in the Methods section, at pH 5.0 and 40 ºC temperature, conditions used for further enzymatic hydrolysis of the pre-treated wheat straw.

The results shown in Table 4 confirm the lack of β-xylosidase and arabinofuranosidase activities in *Pentopan mono conc* contrary to *Ultraflo L* and *Shearzyme 500 L*. β-xylosidase activity was remarkably high for *Shearzyme 500 L* (25 times higher than for *Ultraflo L*) but arabinofuranosidase activity was almost the same in both preparations. Cellulase activity was only detected for *Ultraflo L* whereas β-glucanase activity was detected in the three cocktails. This last activity was nearly 200-fold higher for *Ultraflo L* than for *Shearzyme 500 L*, and almost 360-fold higher for *Ultraflo L* than for *Pentopan mono conc*.

3.3.2. Electrophoresis and zymogram analysis

The purity of the commercial extracts was also analyzed by denaturing polyacrylamide gel electrophoresis (SDS-PAGE) (Fig. 4A). *Ultraflo L* showed up to 10 protein bands with molecular masses ranging from 75 to 20 kDa (Fig. 4A, lane 2), in agreement with the different activities detected here and in other studies for this commercial preparation (Table 3). Major bands migrated to positions corresponding to MWs of 65.8 kDa and 50.4 kDa. On the contrary, *Shearzyme 500 L* had just one major band with a molecular mass of 48.4 kDa (lane 3) and two very faint ones at higher and lower MWs, respectively. For *Pentopan mono conc* (lane 4) two very intense bands, close in size, were detected with Coomassie blue staining (21.9 kDa and 18.3 kDa) along with two faint but sharp bands at 66.2 and 44.1 kDa and a fuzzy protein band between 34 and 26 kDa.

Zymography analysis carried out on SDS-polyacrylamide gels supplemented with 0.5% (w/v) arabinoxylan allowed the detection of endo-xylanase activity (Fig. 4B). For *Shearzyme 500 L* (lane 3) this activity was associated to the 48.4 kDa major protein band. For *Pentopan mono conc* (lane 4) endo-xylanase activity was very intense for the two main bands detected with Coomassie blue staining (Fig. 4A, lane 4). The activity was also linked to the fuzzy band visible at higher MW. For *Ultraflo L* (lane 2) none of the bands detected with Coomassie staining in Fig. 4A (lane 2) showed endo-xylanase activity, although this activity was detected in the aqueous extracts of this commercial preparation (Table 3). This anomaly can occur if the treatment applied to renature the proteins after SDS-PAGE fails. Therefore, we next tried zymography after native polyacrylamide gel electrophoresis (native-PAGE), but the same negative result was obtained (data not shown).

There were also difficulties for renaturing after SDS-PAGE for beta-xylosidase activity visualization. Only with *Shearzyme 500L* was possible to detect activity associated to the major band (data not shown).

In order to avoid renaturation processes after electrophoresis, we carried out isoelectric focusing electrophoresis (IEF) which can help determine both, isoelectric point (pI) and beta-xylosidase activity. MUX staining on IEF gels was performed as described in the method section for beta-xylosidase bands visualization.

Fig. 5 A confirms the presence of a variety of bands in *Ultraflo L* (lane

Table 3
Summary of enzyme cocktails characteristics and optimal conditions.

Enzyme name	*Ultraflo L*	*Shearzyme 500L*	*Pentopan mono conc*
Main activity[a]	β-glucanase and Endo-xylanase	Endo-xylanase	Endo-xylanase
pH[a]	4.5–7.0	4.0–5.0	4.0–6.0
Temperature (°C)[a]	45–60	35–75	45–55
Reported enzyme activities	- β-xylosidase (Sørensen et al., 2007) - α-L-arabinofuranosidase (Sørensen et al., 2007) - cellulase (Truong and Rumpagaporn, 2019) - acetyl esterase (Truong and Rumpagaporn, 2019) - feruloyl esterase (Kim and Lim, 2016; Truong and Rumpagaporn, 2019)	- β-xylosidase (Uçkun Kiran et al., 2013) - α-L-arabinofuranosidase (Uçkun Kiran et al., 2013) - β-glucosidase (Outeiriño et al., 2019; Uçkun Kiran et al., 2013) - cellulase (Outeiriño et al., 2019) - feruloyl esterase (Outeiriño et al., 2019) - β-amylase (Hu et al., 2014) - α-amylase (Hu et al., 2014)	ND[b]

[a] Information supplied by the manufactures.
[b] ND: not described.

Table 4
Protein concentration and specific activities presented in three commercial enzyme preparations at pH 5.0 and 40 °C.

Commercial cocktail	*Ultraflo L*	*Shearzyme 500 L*	*Pentopan mono conc*
[Protein][a]	25.42 ± 0.68	23.13 ± 0.52	0.38 ± 0.01
Specific activity (U/mg protein)[b]			
Endo-xylanase	16.12 ± 0.79	46.74 ± 2.84	339.62 ± 2.78
β-Xylosidase	0.026 ± 0.003	0.671 ± 0.002	ND[c]
Arabinofuranosidase	0.056 ± 0.003	0.052 ± 0.010	ND[c]
Cellulase[d]	0.015 ± 0.001	ND[c]	ND[c]
β-Glucanase	0.359 ± 0.028	0.002 ± 0.000	0.001 ± 0.000

[a] Protein concentration expressed as mean ± standard deviation (n = 3) determined by BCA and expressed in mg/mL for *Ultraflo L* and *Shearzyme 500 L* and mg/mg *for Pentopan mono conc*
[b] Specific activity is expressed as mean ± standard deviation (n = 3)
[c] ND: not detected
[d] FPU units calculated with less than 2 mg of glucose generation.

2) with basic and acidic pIs. None of these bands showed clear β-xylosidase activity after zymography (Fig. 5B, lane 2), but instead, under UV light, fluorescence was seen almost throughout the entire gel lane. Extensive dialysis of the sample did not improve activity visualization (data not shown).

For *Shearzyme 500L* a major protein band was observed, as in SDS-PAGE (Fig. 4A), at pI 5.6 (Fig. 5A, lane3). Beta-xylosidase activity was clearly linked to this band (Fig. 5B, lane 3). This result suggests that the same protein (with MW of 48.4 kDa and pI 5.6) can hydrolyze arabinoxylan and the short substrate MUX. Thus, a single protein may be responsible for the endo-xylanase and beta-xylosidase activity detected in the aqueous extract (Table 4). To our knowledge that fact has not been previously reported. Within the glycoside hydrolase family, the GH43B6 hydrolase from *Paenibacillus curdlanolyticus*, strain B-6, is reported to show multifunctional properties including exo-β-xylosidase, endo-xylanase, and α-arabinofuranosidase enzymatic activities (Wongratpanya et al., 2015).

Pentopan mono conc was solved into three protein bands with pI between 3.6 and 3.3 (Fig. 5A, lane 4), none of them active as beta-xylosidase in the conditions of the experiment. This result confirms the lack of beta-xylosidase in this extract reported in the bibliography and our results (Table 4).

The most common xylanases belong to glycoside hydrolase (GH) family 10 and 11. GH10 family members usually present molecular mass close to 40 kDa in contrast with GH11 which are smaller, close to 20 kDa (Beaugrand et al., 2004). Based on the molecular masses obtained by SDS-PAGE (Fig. 4A) and literature, we classify *Pentopan* endo-xylanase (Sajib et al., 2018) and *Ultraflo L* (Pattarapisitporn et al., 2020; Truong and Rumpagaporn, 2019) into GH11 group. *Shearzyme 500L* endo-xylanase has been categorized as GH10 (Pedersen and Ekloef, 2015).

3.4. Enzymatic hydrolysis of wheat straw

As concluded in Sections 3.1 and 3.2, the solid material resulting after the alkaline treatment with 10 g/L NaOH (WSs_NaOH_{10}) was subjected to enzymatic hydrolysis to evaluate the ability of the three commercial xylanase cocktails to efficiently extract the wheat straw arabinoxylan. The dose of each enzyme was set up considering the endo-xylanase activity at a fixed value of 200 U/g, as the optimum condition defined by Aachary and Prapulla (2009) for corn cob. The degree of extraction and the profile of the monomers generated were analyzed in all cases.

The enzymatic extraction kinetics measured as the generation of ADPs (Fig. 6) showed that the three enzymes tested had similar asymptotic behavior, reaching a plateau around 52 h. The gradual decrease of the extraction rates was not caused by enzymatic inactivation (data not shown). The final yields varied significantly among the commercial cocktails. *Ultraflo L* was positioned as the most efficient cocktail with 59.8 ± 2.5% of extraction, followed by *Pentopan mono conc* and *Shearzyme 500 L* with 51.9 ± 1.6% and 42.5 ± 1.5%, respectively. As expected and described by Andrewartha et al. (1979), the inability of any of the tested enzymes to reach 100% of arabinoxylan extraction reflects the existence in the solid material of a recalcitrant fraction of insoluble arabinoxylan which is not easily accessible to the enzymes. Insoluble arabinoxylan is characterized by having low arabinose:xylose ratios, matching with WSs_NaOH_{10} composition (0.12 A/X ratio). In any case, the hemicellulose extraction here achieved improved significantly compared to those reported for wheat straw (Zhang et al., 2011) and wheat bran (Mathew et al., 2017), and even our pre-treatment with 100 g/L, that only reached 33.5% of extraction in the sample WSl_NaOH_{100} (epigraph 3.1).

Differences in the maximum levels of extraction also reflect the different capabilities of each enzyme to partially overcome the steric hindrances and their different substrate affinity for the chemical structure of the wheat arabinoxylan. These differences are also reflected in the different rates of solubilization.

To explain that, we must consider that different families of glycoside hydrolases have different properties and mechanisms for arabinoxylan degradation. There are some studies comparing GH11 and GH10 endo-xylanases with different solid substrates. Using insoluble highly acetyl-substituted hemicellulose from eucalyptus wood powder (Puchart et al., 2018)' the best results were obtained with the GH10 endo-xylanase, with small differences over the GH11 xylanase assayed. Supporting our results, other authors who worked with pre-treated

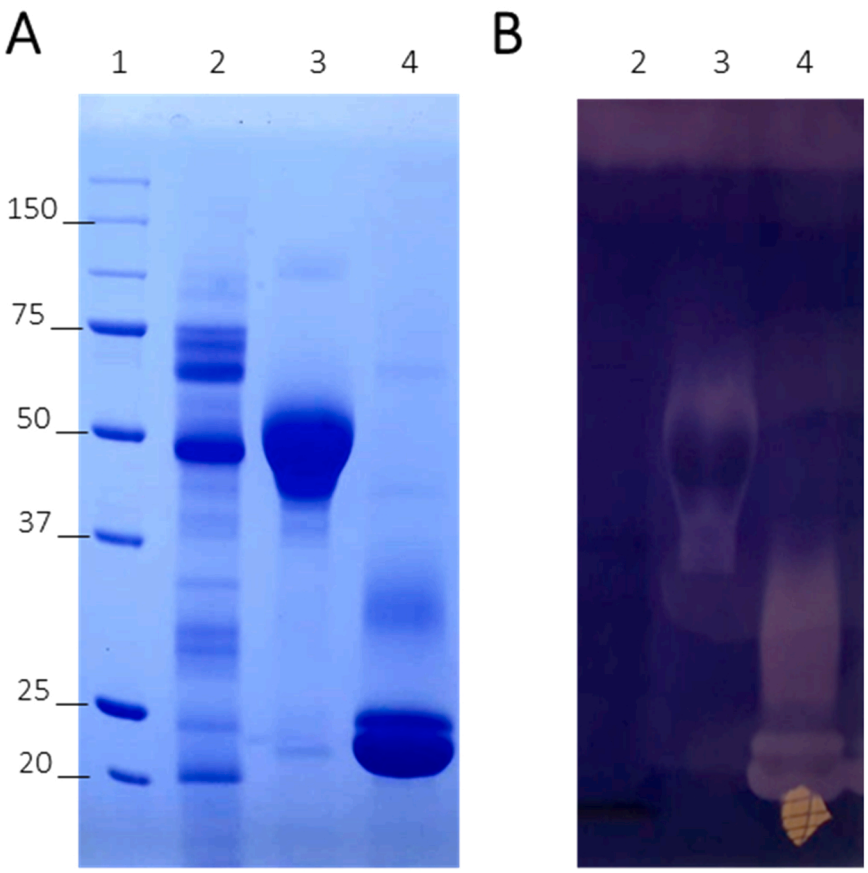

Fig. 4. (A) SDS-PAGE of the commercial enzymes, using 12% polyacrylamide gel and stained with Coomassie blue. Lane 1: Precision plus protein unstained standards. Lane 2: *Ultraflo L,* 20 μg of protein. Lane 3: *Shearzyme 500L,* 20 μg of protein. Lane 4: *Pentopan mono conc,* 20 μg of protein. (B) Zymography analysis using 10% polyacrylamide gel supplemented with 0.5% arabinoxylan and determined with Congo red staining followed by addition of 1 N HCl. Lane 2: *Ultraflo L,* 1.5 endo-xylanase units. Lane 3: *Shearzyme 500 L,* 1.5 endo-xylanase units. Lane 4: *Pentopan mono conc,* 1.5 endo-xylanase units. Samples were boiled for 5 min before SDS-PAGE. After electrophoresis, gel was renatured in 50 mM citrate-phosphate buffer pH 5.0 with 2.5% (v/v) Triton X-100 for 30 min.

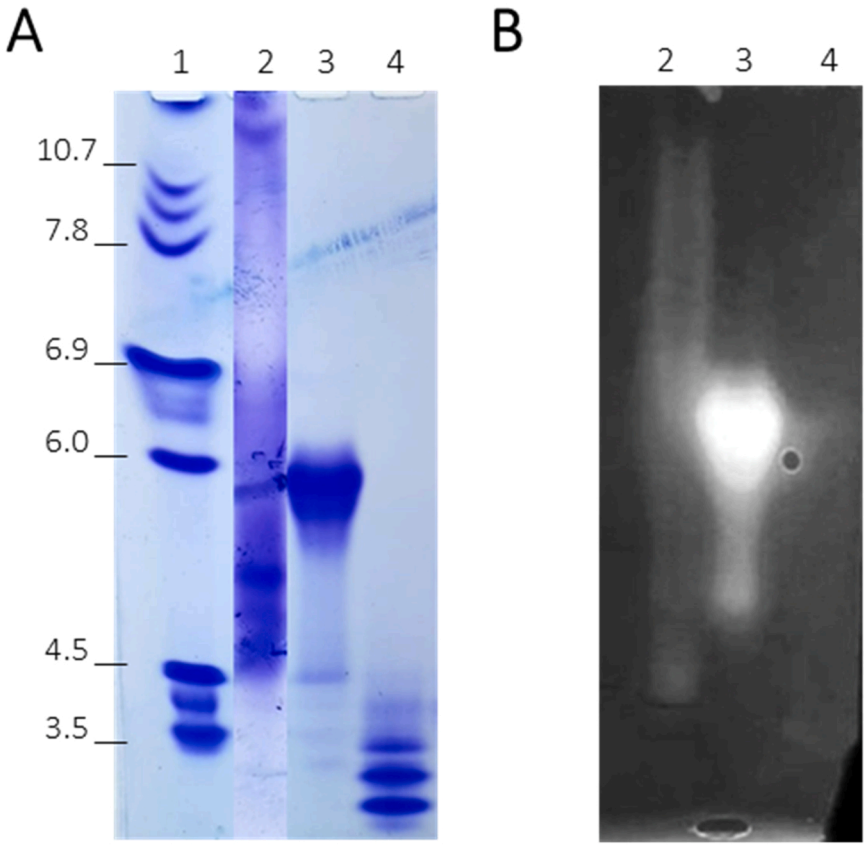

Fig. 5. Isoelectric focusing of the commercial enzymes using Novex pH 3–10 IEF protein gels. (A) Coomassie blue staining. Previous Coomassie staining, the gel was washed with 12% (w/v) trichloroacetic acid. (B) Zymogram for beta-xylosidase activity determination using MUX 40 μM in 50 mM citrate-phosphate buffer pH 5.0 for 30 min at 40 °C. Previous MUX staining, the gel was washed twice with 25% (v/v) 2-propanol for 15 min each and for times with 50 mM citrate-phosphate buffer pH 5.0 for 8 min each. Lane 1: IEF marker 3–10. Lane 2: *Ultraflo L*, 95.3 μg of protein. Lane 3: *Shearzyme 500 L*, 20.1 μg of protein. Lane 4: *Pentopan mono conc*, 10.1 μg of protein.

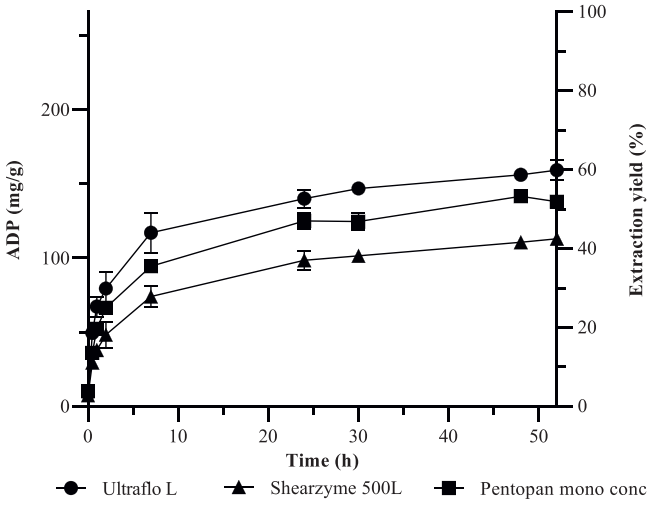

Fig. 6. Evolution of arabinoxylan extraction from WSs_NaOH$_{10}$ due to enzymatic hydrolysis with three commercial enzymes: *Ultraflo L* (•), *Shearzyme 500 L* (▲), and *Pentopan mono conc* (■). ADP was expressed as mg/g of solid, and as extraction yield (%) concerning the total arabinoxylan in the pre-treated material, corresponding 100% to 265.7 mg arabinoxylan/g of solid.

wheat bran, found better performance by GH11 xylanase from *Pentopan Mono BG* on insoluble hemicellulose than the GH10 xylanase (TlXyn11A). The opposite situation happened for the soluble fraction of the arabinoxylan (Mathew et al., 2018).

As a general trend, insoluble arabinoxylan is more efficiently cleaved by GH11 xylanases, which is probably related to their lower size and higher ability to penetrate the solid matrix (Mathew et al., 2018). In the case of soluble xylan, which is characterized by a higher degree of arabinosyl substitutions, GH10 xylanases are better adapted due to their ability to accept substrates with arabinose substituted xylose moieties in its (+1) subsite (Lin et al., 2021).

Looking at our result in Fig. 6, the classification of the *Shearzyme 500L* endo-xylanase as GH10 would justify the lower rate and yield of arabinoxylan extraction achieved (42.5 ± 1.5%) as a result of a lower ability to access through the solid substrate. However, this argument does not explain the different behavior observed between *Ultraflo L* and *Pentopan mono conc* (59.8 ± 2.5% vs 51.9 ± 1.6%, respectively) since both endo-xylanases belong to the same GH11 family. In this case, the superiority of *Ultraflo L* may be related to the action of the accessory activities detected in this cocktail (Table 4), which would act on the arabinoxylan and even on the other polymeric compounds of the solid matrix, contributing to the reduction of the hindrance to the endo-xylanase substrate.

The analysis of the products of these secondary enzymatic activities (shown in Fig. 7) can help to understand these differences. We evaluated the production of xylose and arabinose as the products of mainly β-xylosidase and arabinofuranosidase, respectively. Glucose was considered as a by-product resulting from the primary action of β-glucanase on β-glucans, and the action of cellulases on cellulose. To analyze the release of these monomers we have to take into account that the addition of equal levels of endo-xylanase units leads to differences in the units of the secondary activities. Therefore, we calculated the enzyme units added into the hydrolysis media of WSs_NaOH$_{10}$ with each commercial cocktail by taking into account the measured enzymatic activities reflected in Table 4. Results are shown in Table 5.

We first focused on xylose release. If we consider the β-xylosidase units in each experiment performed with each enzymatic cocktail (Table 5), we should expect the highest levels of the monomer to correspond to the test performed with *Shearzyme 500L*, followed by *Ultraflo L* and finally by *Pentopan mono conc*, with hardly any xylose generation. As shown in Fig. 7A, xylose production was higher for

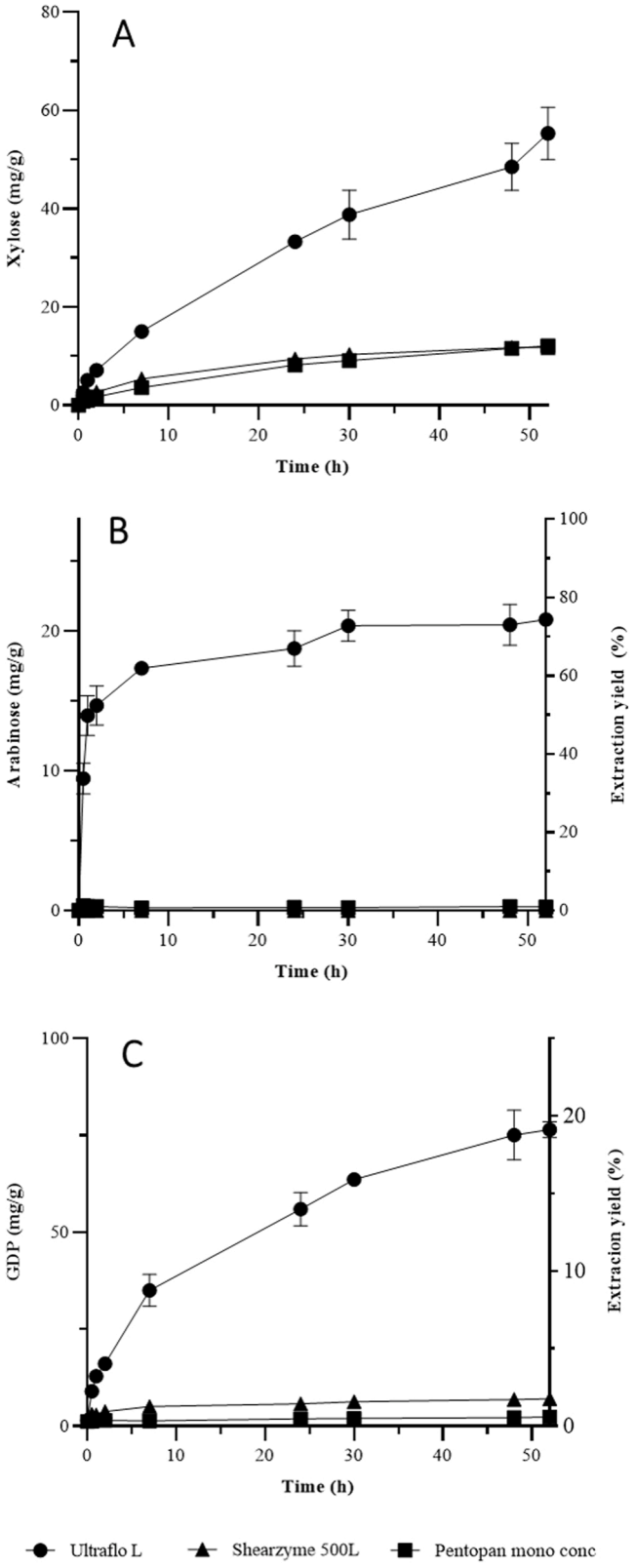

Fig. 7. Evolution in monomer release from WSs_NaOH$_{10}$ thought-out enzymatic hydrolysis with three commercial enzymes: *Ultraflo L* (•), *Shearzyme 500 L* (▲), and *Pentopan mono conc* (■). (A) Xylose release expressed in mg/g of solid; (B) Arabinose release expressed in mg/g solid and % concerning the total composition of WSs_NaOH$_{10}$, corresponding 100% arabinose to 28 mg arabinose/g of solid; (C) GDP release expressed in mg/g solid and % concerning the total composition of WSs_NaOH$_{10}$, corresponding 100% to 400.3 mg glucose/g of solid.

Table 5
Theoretic enzymatic activities (expressed in enzymatic units per gram of solid) that were added for each commercial cocktail in the WSs_NaOH$_{10}$ hydrolysis. Calculated according to the enzymatic activities determined in Table 4.

Commercial cocktail	*Ultraflo L*	*Shearzyme 500 L*	*Pentopan mono conc*
Endo-xylanase (U/g)	200	200	200
β-Xylosidase (U/g)	0.28	2.53	ND[a]
Arabinofuranosidase (U/g)	0.59	0.17	ND[a]
β-Glucanase (U/g)	3.82	< 0.01	< 0.01
Cellulase (U/g)	0.15	ND[a]	ND[a]

[a] ND: not detected.

Ultraflo L, reaching 55.3 ± 5.3 mg/g of the pre-treated wheat straw, which represented around 35% of the total ADPs obtained by this cocktail. Surprisingly, performance for *Shearzyme 500 L* was relatively low in xylose generation compared to *Pentopan mono conc*, with no β-xylosidase activity. These results are in agreement with other works based on these enzymes and other grass lignocellulosic materials. Outeiriño et al., 2019 reported lower xylose release when raw brewery spent grain was hydrolyzed with *Shearzyme 500L* in contrast with *Ultraflo L*. Escarnot et al. (2012) also detected a higher xylose release using *Ultraflo L* in comparison to *Pentopan mono conc* from spelt bran and hull for the same level of arabinoxylan extraction after 4 h with both enzyme cocktails.

As for arabinose (Fig. 7B), *Ultraflo L* differed again considerably from the other two enzymatic cocktails, releasing 75% of the total arabinose in WSs_NaOH$_{10}$. Opposite to *Ultraflo L, Pentopan mono conc* and *Shearzyme 500L* generated less than 1% of arabinose. The relatively good performance of *Ultraflo L* is supported by the high level of arabinofuranosidase. The low production of arabinose by *Shearzyme 500 L* was unexpected.

In terms of GDP, its release was almost negligible for *Pentopan mono conc* and *Shearzyme 500L* (Fig. 7 C). This could be explained by considering the trace levels of cellulase activity detected in these enzymatic cocktails (Table 5). For *Ultraflo L*, 100% of the GDPs released were in their monomeric form. Glucose was expected to be generated mainly from the combined action of β-glucanase in beta-glucan (as the main declared activity for this commercial enzyme), and the β-glucosidase declared as a secondary activity. Glucose could also arise from cellulose as a consequence of the cellulase and β-glucosidase declared activities.

To verify these hypotheses and to identify the source of glucose monomers, the content of the beta-glucan in WSs_NaOH$_{10}$ was analyzed, revealing a very low content of this polysaccharide (around 6.5 mg/g). Composition in beta-glucan cannot explain all the glucose released by *Ultraflo L*. Consequently, these results reflect an intense cellulose degradation by the action of *Ultraflo L*, which accounts for around 18% of extraction of the polymer. The enzymatic hydrolysis of native cellulose is restricted to the amorphous regions, where hemicellulose and cellulose cross-link through hydrogen bonds. In consequence, the enzymatic release of hemicellulose by the action of xylanases makes these amorphous cellulose regions more accessible for cellulases (Xu et al., 2012). Zhang et al. (2011) also described the existence of a synergistic effect of cellulase on the action of xylanase. They attributed this outcome to a layered structure of cellulose and xylan chains occurring alternately in the cell wall substrate. These authors found a linear ratio between xylan and cellulose extraction, which, in our case (see Fig. 8), also appears to happen during the first stages of the process. Nevertheless, linearity disappears in favor of cellulose extraction as the process progresses. This behavior could be explained by suggesting the existence of a threshold fraction of hemicellulose from which the layered structure changes and leaves the remaining cellulose more exposed to the enzymatic attack. In consequence, the activity of the cellulase should be adequately modulated to keep in balance the enhancement of the arabinoxylan extraction and the releasing of cellulose and their products of hydrolysis if they are not desired.

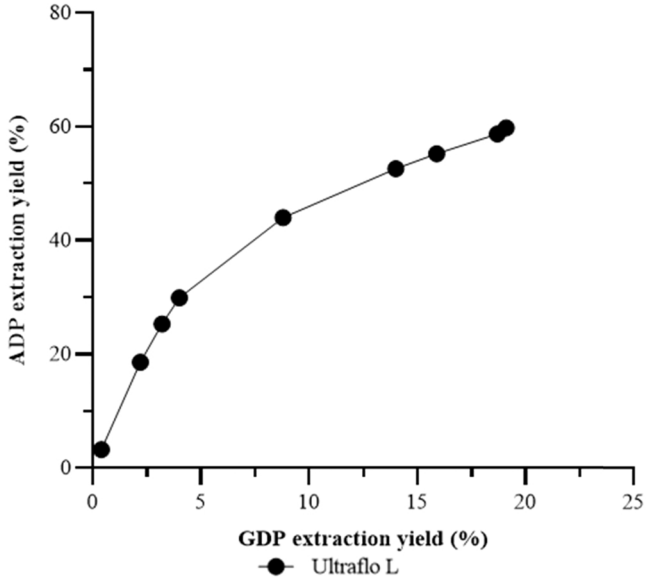

Fig. 8. Relationship between arabinoxylan and cellulose extraction. The calculations were based on the percentage of ADP and GDP released during the hydrolysis of WSs_NaOH$_{10}$ with *Ultraflo L* (•) for 52 h at 40 °C presented in Fig. 6 (ADP extraction yield) and Fig. 7 C (GDP extraction yield).

3.4.1. *Inner structure analysis of the hydrolyzed wheat straw by SEM*

To evaluate the effect produced by the tree enzyme preparations in the disruption of the solid matrix, the inner structure of the hydrolyzed wheat straw was analyzed by SEM.

The comparison between Fig. 2B (corresponding to SEM visualization of WSs_NaOH$_{10}$) and the three images in Fig. 9 shows, first of all, that the enzymes were capable to access and destroy the material even there was 81% of lignin remaining.

But additionally, there is a clear difference between the image corresponding to the solid treated with *Ultraflo L* (Fig. 9A) and the images for *Pentopan mono conc* and *Shearzyme 500 L* treatments (Figs. 9B and 9C). The almost absence in Fig. 9A of the disorganized fibrils that are noticeably seen in the Figs. 9B and 9C appears to reflect the action of cellulase activity of *Ultraflo L* hydrolyzing the less tightened cellulose fractions of the solid material, as suggested before.

Given all, it is reasonable to state that, despite belonging *Pentopan mono conc* and *Ultraflo L* endo-xylanases to the same GH11 family, the best performance of *Ultraflo L* for hemicellulose extraction is due to the action of all accessory enzymes present in this commercial cocktail. These accessory enzymes worked at different levels: arabinofuranosidases, reducing the degree of substitution of the xylan backbone and improving the action of the GH11 endo-xylanase; β-xylosidases, reducing the inhibitory products of endo-xylanases (Rohman et al., 2019); and cellulases, opening the lignocellulosic matrix and improving the accessibility of the endo-xylanase to the inner xylan fibrils.

For general purposes, and about the enzymes here utilized, *Ultraflo L* would be more suitable for those applications based on the monosaccharides (xylose, arabinose, and glucose) recovery for bioethanol or xylitol production. On the other hand, *Pentopan mono conc* and *Shearzyme 500 L* would be better for obtaining ADPs (no in their monomeric form) or xylooligosaccharides for nutraceutical or pharmaceutical uses, although *Ultraflo L* has also been used for both applications: bioethanol and prebiotic production (Escarnot et al., 2012; Pattarapisitporn et al., 2020; Sørensen et al., 2007; Truong and Rumpagaporn, 2019). In any case, analyzing our results, the xylooligosaccharide yields obtained with *Pentopan mono conc* and *Shearzyme 500 L* were higher (120 and 90 mg/g respectively) than those obtained with *Ultraflo L* after subtracting the

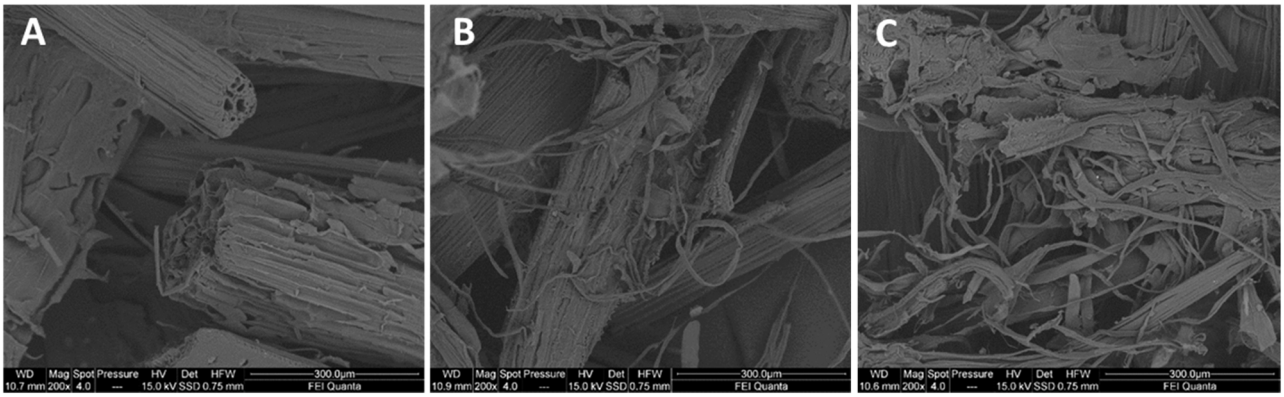

Fig. 9. SEM images of WSs_NaOH$_{10}$ hydrolyzed for 52 h at 40 ºC with three commercial cocktails: (A) 200 U *Ultraflo L*; (B) 200 U *Pentopan mono conc*; (C) 200 U *Shearzyme 500 L*. Scale bar of the images is 300 μm.

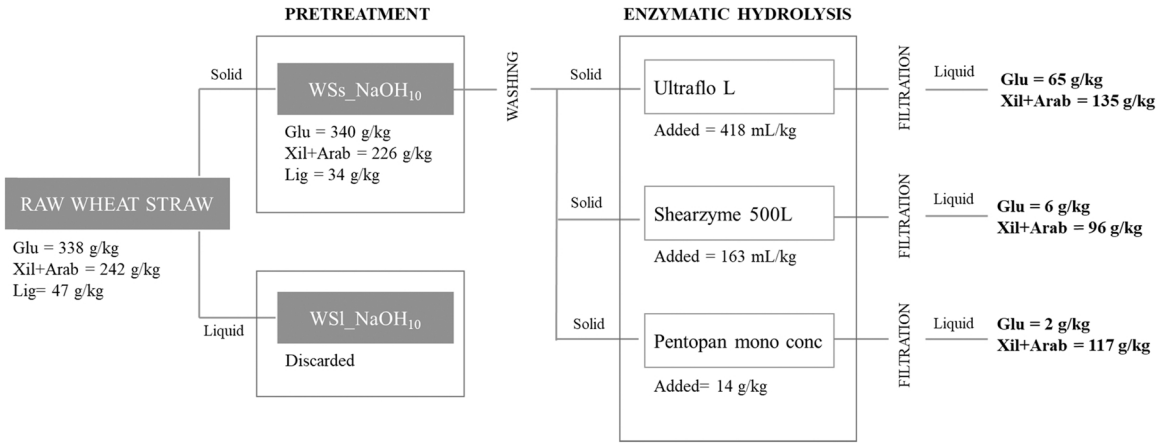

Fig. 10. Flowchart and mass balance of the whole proposed treatment for hemicellulose extraction from wheat straw. Mass of glucose (Glu), xylose and arabinose (Xil+Arab), and lignin (Lig) recovered are shown in g per kg of dry matter. Mass of enzymes added is shown in mL per Kg of dry matter for *Ultraflo L* and *Shearzyme 500 L,* and in g per kg of dry matter for *Pentopan mono conc.*

monosaccharides generated (80 mg/g), which are considered undesirables for prebiotic applications.

The overall results obtained in this exploratory approach indicate that it is possible to obtain acceptable degrees of arabinoxylan extraction (around 50–60%) from wheat straw applying first a mild alkaline pre-treatment and a subsequent enzymatic treatment of the solid with different commercial endo-xylanases. The overall material balance is shown in Fig. 10, where 1 kg of raw wheat straw was considered as a basis for the mass balance calculations. After the pre-treatment with 10 g/L NaOH, 340 g/kg of cellulose (glu) and 226 g/kg hemicellulose (xil+arab) were recovered. With a reasonable quantity of each enzyme cocktail, we were able to release from 96 g/kg to 135 g/kg of the hemicellulose. *Ultraflo L* was able also to extract 65 g/kg cellulose (glu).

The high results achieved, even with the less effective enzyme (*Shearzyme 500 L*) suggest that complete lignin removal is not strictly necessary for the efficient extraction of the hemicellulose from wheat straw. Zhang et al. (2011) also point the beneficial effect provided by the alkaline pre-treatment for breaking down of the ferulate and diferulated bridges that link xylan fibrils with other xylan fibrils and lignin and releasing drastically the acetic moieties that hinder the hydrolysis of the xylan main chain.

As a general conclusion, these results support the potential of enzymes as milder and greener alternatives to harsher thermal and chemical treatments for the effective extraction of the hemicellulosic fraction. The use of new enzymes with improved catalytic properties towards solid substrates and higher temperatures could be a feasible strategy to increase the yield of the process and make it more efficient and suitable to be included in a global bio-refinery strategy for the valorization of wheat straw.

Funding resources

This work was supported by the Spanish Ministry of Science and Innovation (RTI2018–099249-B-I00). Funding for open access charge: Universidade de Vigo/CISUG

CRediT authorship contribution statement

Andrea Rodríguez-Sanz: Methodology, Data curation, Writing – original draft, Writing – review & editing. **Clara Fuciños**: Methodology, Data curation, Project administration. **Ana M. Torrado**: Conceptualization, Methodology, Writing – original draft, Writing – review & editing. **Maria L. Rúa**: Conceptualization, Methodology, Writing – original draft, Writing – review & editing, Project administration.

Declaration of Competing Interest

The authors declare that they have no known competing financial interests or personal relationships that could have appeared to influence the work reported in this paper.

Acknowledgment

Our acknowledgment to Molifibra Molienda y Granulacion S.L. (Castilla y León, Spain) for the supply of free wheat straw samples.

References

Aachary, A.A., Prapulla, S.G., 2009. Value addition to corncob: production and characterization of xylooligosaccharides from alkali pretreated lignin-saccharide complex using Aspergillus oryzae MTCC 5154. Bioresour. Technol. 100, 991–995. https://doi.org/10.1016/j.biortech.2008.06.050.

Adney, B., Baker, J., 2008. Measurement of cellulase activities. Tech. Rep. NREL/TP 510–42628.

Andrewartha, K.A., Phillips, D.R., Stone, B.A., 1979. Solution properties of wheat-flour arabinoxylans and enzymically modified arabinoxylans. Carbohydr. Res. 77, 191–204. https://doi.org/10.1016/S0008-6215(00)83805-7.

Bailey, M.J., Biely, P., Poutanen, K., 1992. Interlaboratory testing of methods for assay of xylanase activity. J. Biotechnol. 23, 257–270. https://doi.org/10.1016/0168-1656(92)90074-J.

Beaugrand, J., Chambat, G., Wong, V.W.K., Goubet, F., Rémond, C., Paës, G., Benamrouche, S., Debeire, P., O'Donohue, M., Chabbert, B., 2004. Impact and efficiency of GH10 and GH11 thermostable endoxylanases on wheat bran and alkali-extractable arabinoxylans. Carbohydr. Res. 339, 2529–2540. https://doi.org/10.1016/j.carres.2004.08.012.

Cano-Ramírez, C., Santiago-Hernández, A., Rivera-Orduña, F.N., Pineda-Mendoza, R.M., Zúñiga, G., Hidalgo-Lara, M.E., 2017. One-step zymogram method for the simultaneous detection of cellulase/xylanase activity and molecular weight estimation of the enzyme. Electrophoresis 38, 447–451. https://doi.org/10.1002/elps.201600347.

Choi, S., Song, C.W., Shin, J.H., Lee, S.Y., 2015. Biorefineries for the production of top building block chemicals and their derivatives. Metab. Eng. 28, 223–239. https://doi.org/10.1016/j.ymben.2014.12.007.

Ebringerová, A., 2005. Structural diversity and application potential of hemicelluloses. Macromol. Symp. 232, 1–12. https://doi.org/10.1002/masy.200551401.

Eisenhuber, K., Jäger, A., Wimberger, J., Karh, H., 2013. Comparison of different pre-treatment methods for separating hemicellulose from straw during lignocellulose bioethanol production. Agron. Res 11, 173–182. https://doi.org/10.1016/j.egypro.2013.08.021.

Escarnot, E., Aguedo, M., Paquot, M., 2012. Enzymatic hydrolysis of arabinoxylans from spelt bran and hull. J. Cereal Sci. 55, 243–253. https://doi.org/10.1016/j.jcs.2011.12.009.

Ewunie, G.A., Yigezu, Z.D., Morken, J., 2021. Biochemical methane potential of Jatropha curcas fruit shell: comparative effect of mechanical, steam explosion and alkaline pretreatments. Biomass-.-. Convers. Biorefinery. https://doi.org/10.1007/s13399-020-01159-1.

Gao, C., Yang, J., Han, L., 2021. Systematic comparison for effects of different scale mechanical-NaOH coupling treatments on lignocellulosic components, micromorphology and cellulose crystal structure of wheat straw. Bioresour. Technol. 326, 124786 https://doi.org/10.1016/j.biortech.2021.124786.

García, J.C., Díaz, M.J., Garcia, M.T., Feria, M.J., Gómez, D.M., López, F., 2013. Search for optimum conditions of wheat straw hemicelluloses cold alkaline extraction process. Biochem. Eng. J. 71, 127–133. https://doi.org/10.1016/j.bej.2012.12.008.

García, M.T., Alfaro, A., Garcia, J.C., Zamudio, M.A.M., Morales, A.B., López, F., 2017. Obtainment of hemicellulose derivatives and cellulose pulp from wheat straw following cold alkaline extraction. Cellul. Chem. Technol. 51, 465–475.

Hernández-Beltrán, J.U., Hernández-De Lira, I., Cruz-Santos, M., Saucedo-Luevanos, A., Hernández-Terán, F., Balagurusamy, N., 2019. Insight into pretreatment methods of lignocellulosic. Appl. Sci. 9, 3721. https://doi.org/10.3390/app9183721.

Hu, S., Dong, J., Fan, W., Yu, J., Yin, H., Shuli, Huang, Liu, J., Shuxia, Huang, Zhang, X., 2014. The influence of proteolytic and cytolytic enzymes on starch degradation during mashing. J. Inst. Brew. 120, 379–384. https://doi.org/10.1002/jib.172.

Ilanidis, D., Stagge, S., Jönsson, L.J., Martín, C., 2021. Hydrothermal Pretreatment of Wheat Straw: Effects of Temperature and Acidity on Byproduct Formation and Inhibition of Enzymatic Hydrolysis and Ethanolic Fermentation. Agronomy 11, 487. https://doi.org/10.3390/agronomy11030487.

Kim, S.M., Lim, S.T., 2016. Enhanced antioxidant activity of rice bran extract by carbohydrase treatment. J. Cereal Sci. 68, 116–121. https://doi.org/10.1016/j.jcs.2016.01.006.

Kontogianni, N., Barampouti, E.M., Mai, S., Malamis, D., Loizidou, M., 2019. Effect of alkaline pretreatments on the enzymatic hydrolysis of wheat straw. Environ. Sci. Pollut. Res. 26, 35648–35656. https://doi.org/10.1007/s11356-019-06822-3.

Kristensen, J.B., Thygesen, L.G., Felby, C., Jørgensen, H., Elder, T., 2008. Cell-wall structural changes in wheat straw pretreated for bioethanol production. Biotechnol. Biofuels 1, 1–9. https://doi.org/10.1186/1754-6834-1-5.

Laemmli, U.K., 1970. Cleavage of structural proteins during the assembly of the head of acteriophage. Nature 227 (680–685), T4.

Lin, S., Agger, J.W., Casper, W., Meyer, A.S., 2021. Feruloylated Arabinoxylan and Oligosaccharides: Chemistry, Nutritional Functions, and Options for Enzymatic Modification. Annu. Rev. Food Sci. Technol. 25, 331–354. https://doi.org/10.1146/annurev-food-032818-121443.

Linares-Pasten, J.A., Aronsson, A., Karlsson, E.N., 2016. Structural Considerations on the Use of Endo-Xylanases for the Production of prebiotic Xylooligosaccharides from Biomass. Curr. Protein Pept. Sci. 19, 48–67. https://doi.org/10.2174/1389203717666160923155209.

Mathew, S., Aronsson, A., Karlsson, E.N., Adlercreutz, P., 2018. Xylo- and arabinoxylooligosaccharides from wheat bran by endoxylanases, utilisation by probiotic bacteria, and structural studies of the enzymes. Appl. Microbiol. Biotechnol. 102, 3105–3120. https://doi.org/10.1007/s00253-018-8823-x.

Mathew, S., Karlsson, E.N., Adlercreutz, P., 2017. Extraction of soluble arabinoxylan from enzymatically pretreated wheat bran and production of short xylo-oligosaccharides and arabinoxylo-oligosaccharides from arabinoxylan by glycoside hydrolase family 10 and 11 endoxylanases. J. Biotechnol. 260, 53–61. https://doi.org/10.1016/j.jbiotec.2017.09.006.

McIntosh, S., Vancov, T., 2011. Optimisation of dilute alkaline pretreatment for enzymatic saccharification of wheat straw. Biomass-.-. Bioenergy 35, 3094–3103. https://doi.org/10.1016/j.biombioe.2011.04.018.

Nordberg Karlsson, E., Schmitz, E., Linares-Pastén, J.A., Adlercreutz, P., 2018. Endo-xylanases as tools for production of substituted xylooligosaccharides with prebiotic properties. Appl. Microbiol. Biotechnol. 102, 9081–9088. https://doi.org/10.1007/s00253-018-9343-4.

Outeiriño, D., Costa-Trigo, I., Pinheiro de Souza Oliveira, R., Pérez Guerra, N., Domínguez, J.M., 2019. A novel approach to the biorefinery of brewery spent grain. Process Biochem 85, 135–142. https://doi.org/10.1016/j.procbio.2019.06.007.

Overend, R.P., Chornet, E., 1987. Fractionation of lignocellulosics by steam-aqueous pretreatments. Philosophical Transactions of the Royal Society of London. Series A, Mathematical and Physical Sciences 321, 523–536. https://doi.org/10.1098/rsta.1987.0029.

Pattarapisitporn, A., Jaichakan, P., Klangpetch, W., 2020. Oligosaccharides from rice straw and rice husks produced by glycoside hydrolase family 10 and 11 xylanases. Asia-Pacific. J. Sci. Technol. 25, 1–8.

Pedersen, M., Viksø-Nielsen, A., Meyer, A.S., 2010. Monosaccharide yields and lignin removal from wheat straw in response to catalyst type and pH during mild thermal pretreatment. Process Biochem 45, 1181–1186. https://doi.org/10.1016/j.procbio.2010.03.020.

Pedersen, S., Ekloef, J., 2015, Process for producing ethanol from starch using a GH5 xylanase (Patent No. WO 2016/005521 A1). Novozymes A/S.

Peng, Y., Wu, S., 2010. The structural and thermal characteristics of wheat straw hemicellulose. J. Anal. Appl. Pyrolysis 88, 134–139. https://doi.org/10.1016/j.jaap.2010.03.006.

Pinales-Márquez, C.D., Rodríguez-Jasso, R.M., Araújo, R.G., Loredo-Treviño, A., Nabarlatz, D., Gullón, B., Ruiz, H.A., 2021. Circular bioeconomy and integrated biorefinery in the production of xylooligosaccharides from lignocellulosic biomass: A review. Ind. Crops Prod. 162. https://doi.org/10.1016/j.indcrop.2021.113274.

Poletto, P., Pereira, G.N., Monteiro, C.R.M., Pereira, M.A.F., Bordignon, S.E., de Oliveira, D., 2020. Xylooligosaccharides: Transforming the lignocellulosic biomasses into valuable 5-carbon sugar prebiotics. Process Biochem 91, 352–363. https://doi.org/10.1016/j.procbio.2020.01.005.

Puchart, V., Fraňová, L., Mørkeberg Krogh, K.B.R., Hoff, T., Biely, P., 2018. Action of different types of endoxylanases on eucalyptus xylan in situ. Appl. Microbiol. Biotechnol. 102, 1725–1736. https://doi.org/10.1007/s00253-017-8722-6.

Robak, K., Balcerek, M., 2020. Current state-of-the-art in ethanol production from lignocellulosic feedstocks. Microbiol. Res. 240, 126534 https://doi.org/10.1016/j.micres.2020.126534.

Rohman, A., Dijkstra, B.W., Puspaningsih, N.N.T., 2019. β-xylosidases: Structural diversity, catalytic mechanism, and inhibition by monosaccharides. Int. J. Mol. Sci. 20, 7–11. https://doi.org/10.3390/ijms20225524.

Ruzene, D.S., Silva, D.P., Vicente, A.A., Gonçalves, A.R., Teixeira, J.A., 2008. An alternative application to the Portuguese agro-industrial residue: Wheat straw. Appl. Biochem. Biotechnol. 147, 85–96. https://doi.org/10.1007/s12010-007-8066-2.

Sajib, M., Falck, P., Sardari, R.R.R., Mathew, S., Grey, C., Karlsson, E.N., Adlercreutz, P., 2018. Valorization of Brewer's spent grain to prebiotic oligosaccharide: Production, xylanase catalyzed hydrolysis, in-vitro evaluation with probiotic strains and in a batch human fecal fermentation model. J. Biotechnol. 268, 61–70. https://doi.org/10.1016/j.jbiotec.2018.01.005.

Santibáñez, L., Henríquez, C., Corro-Tejeda, R., Bernal, S., Armijo, B., Salazar, O., 2021. Xylooligosaccharides from lignocellulosic biomass: A comprehensive review. Carbohydr. Polym. 251. https://doi.org/10.1016/j.carbpol.2020.117118.

Saulnier, L., Crépeau, M.J., Lahaye, M., Thibault, J.F., Garcia-Conesa, M.T., Kroon, P.A., Williamson, G., 1999. Isolation and structural determination of two 5,5′-diferuloyl oligosaccharides indicate that maize heteroxylans are covalently cross-linked by oxidatively coupled ferulates. Carbohydr. Res. 320, 82–92. https://doi.org/10.1016/S0008-6215(99)00152-4.

Shallom, D., Shoham, Y., 2003. Microbial hemicellulases. Curr. Opin. Microbiol. 6, 219–228. https://doi.org/10.1016/S1369-5274(03)00056-0.

Sluiter, A., Hames, B., Ruiz, R., Scarlata, C., Sluiter, J., Templeton, D., Crocker, D., 2012. Determination of structural carbohydrates and lignin in Biomass. Tech. Rep. NREL/TP 510–42618.

Sørensen, H.R., Pedersen, S., Meyer, A.S., 2007. Synergistic enzyme mechanisms and effects of sequential enzyme additions on degradation of water insoluble wheat arabinoxylan. Enzym. Microb. Technol. 40, 908–918. https://doi.org/10.1016/j.enzmictec.2006.07.026.

Svärd, A., Brännvall, E., Edlund, U., 2017. Rapeseed straw polymeric hemicelluloses obtained by extraction methods based on severity factor. Ind. Crops Prod. 95, 305–315. https://doi.org/10.1016/j.indcrop.2016.10.038.

Tang, W., Wu, X., Huang, C., Ling, Z., Lai, C., Yong, Q., 2021. Natural surfactant-aided dilute sulfuric acid pretreatment of waste wheat straw to enhance enzymatic hydrolysis efficiency. Bioresour. Technol. 324, 124651 https://doi.org/10.1016/j.biortech.2020.124651.

Terrett, O.M., Dupree, P., 2019. Covalent interactions between lignin and hemicelluloses in plant secondary cell walls. Curr. Opin. Biotechnol. 56, 97–104. https://doi.org/10.1016/j.copbio.2018.10.010.

Thorenz, A., Wietschel, L., Stindt, D., Tuma, A., 2018. Assessment of agroforestry residue potentials for the bioeconomy in the European Union. J. Clean. Prod. 176, 348–359. https://doi.org/10.1016/j.jclepro.2017.12.143.

Truong, K.T.P., Rumpagaporn, P., 2019. Oligosaccharides preparation from rice bran arabinoxylan by two different commercial endoxylanase enzymes. J. Nutr. Sci. Vitaminol. (Tokyo). 65, S171–S174. https://doi.org/10.3177/jnsv.65.S171.

Uçkun Kiran, E., Akpinar, O., Bakir, U., 2013. Improvement of enzymatic xylooligosaccharides production by the co-utilization of xylans from different origins. Food Bioprod. Process. 91, 565–574. https://doi.org/10.1016/j.fbp.2012.12.002.

Van Dyk, J.S., Pletschke, B.I., 2012. A review of lignocellulose bioconversion using enzymatic hydrolysis and synergistic cooperation between enzymes-Factors affecting enzymes, conversion and synergy. Biotechnol. Adv. 30, 1458–1480. https://doi.org/10.1016/j.biotechadv.2012.03.002.

Wongratpanya, K., Imjongjairak, S., Waeonukul, R., Sornyotha, S., Phitsuwan, P., Pason, P., Nimchua, T., Tachaapaikoon, C., Ratanakhanokchai, K., 2015. Multifunctional properties of glycoside hydrolase family 43 from Paenibacillus curdlanolyticus strain B-6 including exo-β-xylosidase, endo-xylanase, and α-L-arabinofuranosidase activities. BioResources 10, 2492–2505. https://doi.org/10.15376/biores.10.2.2492-2505.

Xu, N., Zhang, W., Ren, S., Liu, F., Zhao, C., Liao, H., Xu, Z., Huang, J., Li, Q., Tu, Y., Yu, B., Wang, Y., Jiang, J., Qin, J., Peng, L., 2012. Hemicelluloses negatively affect lignocellulose crystallinity for high biomass digestibility under NaOH and H 2SO 4 pretreatments in Miscanthus. Biotechnol. Biofuels 5, 1–12. https://doi.org/10.1186/1754-6834-5-58.

Yan, Q.J., Wang, L., Jiang, Z.Q., Yang, S.Q., Zhu, H.F., Li, L.T., 2008. A xylose-tolerant β-xylosidase from Paecilomyces thermophila: Characterization and its co-action with the endogenous xylanase. Bioresour. Technol. 99, 5402–5410. https://doi.org/10.1016/j.biortech.2007.11.033.

Zhang, J., Siika-Aho, M., Tenkanen, M., Viikari, L., 2011. The role of acetyl xylan esterase in the solubilization of xylan and enzymatic hydrolysis of wheat straw and giant reed. Biotechnol. Biofuels 4. https://doi.org/10.1186/1754-6834-4-60.